NOVARTIS

S1P-S1PR1 activity controls VEGF-A signaling during lymphatic vessel development

Running title: S1PR1 is required for lymphangiogenesis

Golding-Ochsenbein AM*, Vidal S, Wilmering Wetter B, Guibourdenche C, Beerli C, Chang L, Leonhard S, Holway N, Seuwen K, Jurisic G*

Novartis Institutes for BioMedical Research, Novartis Pharma AG, Basel, Switzerland

* Corresponding authors

1   **Abstract**

2

3   Sphingosine-1-phosphate (S1P), a lipid signaling molecule produced by endothelial cells,

4   is required for development and homeostasis of blood vessels. However, its role during

5   lymphatic vessel development is unclear. We show in murine newborns that pharmaco-

6   logically enhanced S1P signaling increases VEGF-A-dependent LEC proliferation. In con-

7   trast, S1PR1 inhibition, mediated by the antagonist NIBR0213 or LEC-specific genetic

8   deletion of *S1pr1,* promotes filopodia formation and vessel branching, independent of

9   VEGF-A. To investigate the S1P and VEGF-A signaling crosstalk observed *in vivo*, we

10   used LECs cultured *in vitro.* We demonstrate that S1P activates endogenous S1PR1 in

11   a constitutive, autocrine manner. Importantly, S1P-S1PR1 activity was required for

12   VEGF-A-induced LEC proliferation and strongly supported ERK1/2 activation and

13   VEGFR-2 trafficking to the perinuclear area. In conclusion, S1P-S1PR1 signaling pro-

14   motes VEGF-A-dependent LEC proliferation and limits migratory and filopodia-forming

15   responses. Hence, S1P-S1PR1 signaling is required for balanced growth factor-induced

16   lymphangiogenesis and correctly patterned lymphatic vessels during postnatal develop-

17   ment.

Introduction

Lymphangiogenesis, the formation of new lymphatic vessels from pre-existing ones, is orchestrated by tissue-derived growth factors such as VEGF-C and VEGF-A, and by cell intrinsic mechanisms (Vaahtomeri et al., 2017) that create a balance between proliferating and migratory, filopodia-forming lymphatic endothelial cells (LECs) (James et al., 2013). This balance is key to subsequent vascular patterning events such as branching and hence, influence lymphatic vessel morphology (Gerhardt et al., 2003). Interestingly, VEGF-A is known to enhance proliferation and less so sprouting (Nagy et al., 2002; Wirzenius et al., 2007), whereas VEGF-C induces both sprouting and proliferation.

VEGF-A activates the receptor VEGFR-2, whereas VEGF-C, in its processed form, activates both VEGFR-2 and VEGFR-3. The latter receptor is critically required for lymphangiogenesis. Both receptors belong to the receptor tyrosine kinase family, and ligand activation leads to dimerization and auto-phosphorylation, followed by internalization (reviewed in (Zhang and Simons, 2014)) and fusion with endosomal compartments (Simons et al., 2016; Zhang and Simons, 2014). These events are important for the activation of several downstream signaling pathways including ERK1/2 that is crucial for endothelial cell function (Simons et al., 2016).

Sphingosine-1-phosphate (S1P), a lipid mediator secreted by erythrocytes, platelets and endothelial cells, signals via 5 specific G protein-coupled receptors (S1PR1-5) by inducing their internalization and activating downstream signaling cascades (Mullershausen et al., 2009; Yanagida and Hla, 2017). S1PR1, highly expressed by endothelial cells, is crucial for embryonic blood vessel development and function (Yanagida and Hla, 2017). It

1

1   stabilizes endothelial barrier and negatively regulates blood endothelial cell sprouting

2   (Ben Shoham et al., 2012; Bigaud et al., 2016; Gaengel et al., 2012; Jung et al., 2012).

3   However, opposing conclusions of S1P acting either pro- or anti-angiogenic were previ-

4   ously made (Ben Shoham et al., 2012; Caballero et al., 2009; English et al., 2001; English

5   et al., 2000; Gaengel et al., 2012; Licht et al., 2003). For lymphatic vessels, S1P was

6   reported to promote lymphangiogenesis in a matrigel plug assay in adult mice (Yoon et

7   al., 2008). Additionally, sphingosine kinase activity in LECs was shown to be required for

8   generation of S1P and proper lymphatic vessel patterning and arrangement of cell junc-

9   tions *in vivo* (Pham et al., 2010). However, the mechanism of how S1P affects lymphatic

10   vessel development, in particular its effect on growth factor signaling, and the role of

11   S1PR1 during this process are not known.

12   We show here, for the first time, that S1P-S1PR1 activity influences lymphangiogenesis

13   by promoting VEGF-A-dependent LEC proliferation and by limiting migratory and filopo-

14   dia-forming responses. Furthermore, antagonism of S1PR1 leads to dysfunctional lym-

15   phatic vessels. Hence, S1P-S1PR1 signaling is required for the correct patterning and

16   maintenance of function of the lymphatic vessel network during postnatal development.

17

1 **Methods**

2

3 *Endothelial cell culture*

4 Primary adult human dermal LECs (PromoCell) or human umbilical vein endothelial cells

5 (HUVECs) (PromoCell) were cultured on plates coated with 50 μg/ml Purecol collagen

6 type I (Advanced Biomartix) and in EGM-MV medium without VEGF-A (PromoCell). For

7 starvation of the cells, EBM-MV (PromoCell) without FCS was used. For washing steps

8 pH7.4 phosphate-buffered saline (PBS) without $CaCl_2$ and $MgCl_2$ (Gibco) was used. Cells

9 were treated with the dual non ATP-competitive sphingosine kinase inhibitor SKI-II

10 (SIGMA), S1P (Avanti Polar) diluted in 90% DMSO containing 50 mM HCl, NIBR0213

11 (Novartis) and recombinant carrier-free human VEGF-A165 (R&D systems).

12

13 *Measurements of S1P concentration*

14 S1P concentrations were measured as previously described (Billich et al., 2013). To re-

15 duce unspecific binding, extracts were subjected to acetylation as described

16 in (Berdyshev et al., 2005). Sphingosine derivatives were detected in positive mode; neg-

17 ative ionization was used for S1P. Quantification was performed based on the area ratios

18 of the compound over internal standard in the extracted ion chromatograms. Recovery

19 was >86% for all analytes. The limit of quantification, as determined by the lowest cali-

20 bration sample showing signal-to-noise ratio >5 and accuracy <14%, was 0.5 ng/ml for

21 Sph, 0.1 ng/ml for S1P.

22

1   *Electric Cell-substrate Impedance Sensing (ECIS)*

2   The lymphatic endothelial cell barrier tightness was assessed using an ECIS® ZΘ instru-

3   ment with a 16-well array station (Applied Biophysics). 8-well chamber slides (8W10E+,

4   ibidi) were pre-incubated with 50 µg/ml fibronectin (Roche) and then washed with sterile

5   H_2O. Next, 30000 adult human dermal LECs per well were plated in EGM and impedance

6   values were recorded at 4,000 Hz every 30 seconds. When a monolayer with stable im-

7   pedance levels of 3000-3500 ohm was formed, treatments with compounds started. To

8   investigate LEC endogenous S1P functions, 10 μM SKI-II or DMSO control was spiked

9   into corresponding wells. After 4 h cells were washed with PBS and starved in EBM con-

10   taining again 10 μM SKI-II for 3 h. Next, cells were treated ± 1 µM S1P, S1P+0.3 µM

11   NIBR0213 or DMSO control. To rule out NIBR0213 toxic effects, 0.1 or 0.01 µM

12   NIBR0213 was spiked into corresponding wells. After 5 h 10 µM S1P or DMSO control

13   were spiked into corresponding wells. Graphs were generated using TIBCO Spotfire

14   6.5.3. Impedance curves were normalized to DMSO control.

15

16   *Immunofluorescent approaches for in vitro experiments*

17   Cells were starved for 4 h or overnight in medium without FCS and received indicated

18   treatments for indicated times. Then cells were fixed with 4% PFA for 10 min at room

19   temperature and washed with PBS before blocking for 1 h in immunomix (PBS containing

20   5 % donkey serum, 1 % bovine serum albumin (BSA) and 0.1 % Triton-X). The following

21   antibodies were incubated overnight at 4°C: rat anti-human CD31 (DAKO, M082329-2),

22   rabbit anti-human S1PR1 (Santa Cruz, sc-25489), goat anti-human VEGFR-2 (R&D sys-

23   tems, AF357), rabbit anti-human Rab5 (Cell Signaling, #3547P). After an intense wash

1 step in 0.1% Triton-X PBS, samples were incubated for 1 h at room temperature with

2 Alexa Fluor 488, 594 or 647 nm-conjugated secondary antibodies (Invitrogen). Samples

3 were imaged with a Zeiss LSM 700 (Zeiss) confocal microscope using the Zen 2011 SP3

4 (black edition) software or for VEGFR-2 trafficking with a Yokogawa CV7000 system us-

5 ing the CellVoyager R1.17.05 software. Yokogawa images were analyzed with ImageJ:

6 The perinuclear area was defined by Hoechst area plus a 1.625 μm radius and total cell

7 area was defined based on CD31 plasma membrane staining. Total cell VEGFR-2 was

8 defined as 100%. Values were normalized to DMSO control.

9

10 *Homogeneous time resolved fluorescence (HTRF)*

11 HTRF approaches (Cisbio) were used to determine VEGFR-2 pTyr1175 and ERK

12 pThr202/Tyr204 levels. To measure VEGFR-2 pTyr1175 levels after VEGF-A stimulation

13 with or without S1PR1 pathway modulation, 40000 cells per 96 well were seeded in EGM

14 in the morning. In the evening, cells were washed with PBS and starved overnight in EBM

15 without FCS. Next, cells were stimulated with the indicated treatments for 2 and 5 min

16 and 2 h before processing according to manufacturer's instructions. For determination of

17 pERK1/2 levels in the presence or absence of SKI-II, 20000 human dermal LECs per 96

18 well were seeded in EGM. The next day 10 μM SKI-II was spiked into corresponding wells

19 and incubated for 4 h before EGM removal, a PBS wash and the addition of EBM starva-

20 tion medium without FCS ± 10 μM SKI-II. Cells were starved for 3 h before 10 min stimu-

21 lation with the indicated treatments. Next, cells were processed according to manufac-

22 turer's instructions. Fluorescent signals were measured with TRF Light Unit EnVision

23 (PerkinElmer). EC_{50} and E_{max} were calculated with Prism 6 (GraphPad Software).

1   *Cell proliferation assay*

2   For the 5-ethynyl-2´-deoxyuridine (EdU) proliferation assay, 5000 LEC per well of a 96

3   well plate were seeded in EGM in the morning. In the evening, cells were washed with

4   PBS before an overnight starvation in EBM. The next morning, cells were treated with

5   100 ng/ml VEGF-A ± 0.3 μM NIBR0213 or DMSO control and in the evening 10 μM EdU

6   was spiked. 24 h after the addition of VEGF-A cells were fixed with 4 % PFA before further

7   processing according to the Click-iT EdU Imaging Kit (Invitrogen). Experiments were per-

8   formed with eight replicates per group. Per well nine non-overlapping images were ac-

9   quired and analyzed with the Operetta High Content Screening System microscope

10   (PerkinElmer) and Harmony 4.1 software.

11

12   *Mice*

13   For *in vivo* experiments with pharmacological approaches C57BL/6 females were pur-

14   chased from Charles River Laboratories (France) or came from Novartis Pharma AG Ba-

15   sel internal breeding facilities. For lymphatic vessel-specific depletion of S1PR1, the well-

16   established mouse lines Prox-1creERT2 mice (Bazigou et al., 2011) and S1PR1 floxed

17   mice (Allende et al., 2003) were crossed and bred in the animal breeding facility of No-

18   vartis Pharma AG, Basel. For pharmacological approaches C57BL/6 pups received i.p. 4

19   or 20 mg/kg/day Compound 31 (Cmpd 31) (Novartis) diluted in PEG200/5% glucose

20   (70/30%) or PBS/PEG200/5% glucose (50%/35%/15%) for co-treatments, 3 or 6

21   mg/kg/day VEGF-A neutralizing antibody 4G3 (Novartis) diluted in PBS/PEG200/5% glu-

22   cose (50%/35%/15%), 1, 5 or 10 mg/kg/day NIBR0213 (Novartis) diluted in PEG200/5%

23   glucose (70/30%) or PBS/PEG200/5% glucose (50%/35%/15%) for co-treatments with

6

1   4G3 (6 mg/kg/day) from postnatal day (P) 0.5 to P3.5 and were sacrificed at P4.5. To

2   induce recombination events, homozygous *S1pr1* flx and *Prox-1-CreERT2+* (S1PR1-

3   iΔLEC) or *Prox-1-CreERT2-* (control) littermates received intragastric injections of 50 μg

4   tamoxifen (Sigma), dissolved in EtOH and sunflower seed oil (Sigma) from P1 to P4.

5   Tissues were harvested at P7 to allow enough time for recombination to occur.

6

7   *Animal study approval*

8   All *in vivo* experiments were approved by the Cantonal Veterinary Office Basel-Stadt (li-

9   cense number BS-2586).

10

11   *Whole-mount staining and morphometric analyses*

12   Abdominal skin or diaphragms were harvested and skin samples were incubated for 1 h

13   in 20 mM EDTA at 37°C to facilitate the removal of the epidermis. Then tissues were fixed

14   for 2 h in freshly prepared 4% PFA at 4°C. Next, samples were washed in PBS and

15   blocked in immunomix (described above) for 1 h at RT before overnight primary antibody

16   incubation at RT. The following primary antibodies were used: rat-anti mouse S1PR1

17   (R&D Systems, MAB7089), hamster anti-mouse CD31 (Millipore, MAB1398Z), goat anti-

18   mouse Prox-1 (R&D Systems, AF2727), rabbit anti-mouse LYVE1 (AngioBio, 11-034),

19   goat anti-mouse LYVE1 (R&D Systems, AF2125), rabbit anti-mouse KI-67 (Neomarkers,

20   RM-9106-S1), goat anti-mouse VEGFR-2 (R&D Systems, AF644). The next day, whole

21   mounts were washed and incubated for 2 hours with AlexaFluor 488, 594 or 647-conju-

22   gated secondary antibodies (all from Invitrogen) at RT. Whole-mount z-stacks were ac-

23   quired on a Zeiss LSM 700 confocal microscope with the Zen 2011 SP3 (black edition)

1   software. Images were processed with Zen software. For lateral diaphragm segments

2   images were processed with a personalized Fiji macro (Schindelin et al., 2012) (Rueden

3   et al., 2017). The macro automated the following tasks: the maximum intensity projection

4   of each image stack was calculated and then each projection was stitched together using

5   Fiji's Grid/Collection stitching plugin (Preibisch et al., 2009). The stitched image was then

6   thresholded using Fiji's default (IsoData) algorithm (Ridler and Calvard, 1978) and auto-

7   matic threshold value, colored green and then saved. The macro is freely available at

8   https://github.com/Novartis/ExactAddressTBC. Lateral diaphragm segments were ana-

9   lyzed as described previously (Ochsenbein et al., 2016). Other images were analyzed by

10   hand with ImageJ.

11

12   *Quantification of lymphangiogenic growth factor levels in P2.5 diaphragms*

13   To assess growth factor levels in postnatal diaphragms, tissues were collected and

14   mRNA levels were assessed by qPCR. To do so, two diaphragms of P2.5 C57Bl6 pups

15   were collected in RNA later (Qiagen) before they were processed in RLT buffer containing

16   1% mercaptoethanol (Sigma) with the help of metal beads (MP Biomedicals) and the

17   FastPrep-24 tissue ruptor (MP Biomedicals). Next, RNA was extracted according to the

18   RNeasy Micro Kit (Qiagen). The RNA was transcribed to cDNA using the High-Capacity

19   cDNA Reverse Transcription Kit (Applied Biosystems). The PCR reactions were per-

20   formed using a Quant Studio 7 Flex Fast Real-Time PCR System (Applied Biosystems

21   by life technologies) and the following Taqman primers (Thermo Fisher): *Actb*

22   (Mm02619580_g1), *Vegf-A* (Mm00437306_m1), *Vegf-C* (Mm00437310_m1), *Vegf-D*

23   (Mm01131929_m1). Data is presented by fold change to *Actb*.

1

2 *Statistical data analysis*

3 Statistical analyses were performed using Prism 7 (GraphPad Software). Data are shown

4 as mean ± standard deviation. Normal distribution was tested with Shapiro-Wilk test. Nor-

5 mally distributed data were analyzed using the student's t-test or, for comparisons of

6 means of more groups, one-way ANOVA and Dunnett's test were used. For non-normal

7 distributed data non-parametric tests where used. Statistical significance is indicated by

8 asterisks: * $p < 0.05$, ** $p < 0.01$, *** $p < 0.001$, **** $p < 0.0001$. Differences were consid-

9 ered statistically significant when $p < 0.05$.

10

11

1   **Results**

2

3   *Increasing tissue S1P levels enhances lymphatic endothelial cell proliferation in vivo in a*

4   *VEGF-A-dependent manner*

5   To study the role of S1P in early postnatal lymphangiogenesis, we used a previously

6   established murine model where lymphatic vessels on the pleural side of the diaphrag-

7   matic muscle are monitored (Ochsenbein et al., 2016). In a first series of experiments we

8   enhanced S1P signaling by treating pups from postnatal day (P) 0.5-3.5 with Cmpd 31, a

9   highly specific S1P lyase inhibitor that increases S1P concentrations *in vivo* (Weiler et al.,

10   2014). At P4.5, LYVE1+ lymphatic vessels expressed S1PR1, which was also present on

11   some single cells and on CD31+ blood vessels (Fig. 1A). Intraperitoneal injection of 20

12   mg/kg/day of Cmpd 31 significantly increased S1P levels in muscle tissue (Fig. S1A) and,

13   in the diaphragm, lymphatic vessel diameters and lymphatic endothelial cell (LEC) prolif-

14   eration (assessed as %KI-67+ cells per PROX-1+ cells) without changing the vessel

15   branching response (Fig 1B-E,G,H). Thus, we conclude that enhanced S1P signaling

16   boosts LEC proliferation during postnatal development.

17   Next, we asked whether S1P might increase lymphatic vessel diameter and cell prolifer-

18   ation via cross-talk with VEGFR-2, as reported for blood endothelial cells (Gaengel et al.,

19   2012). Indeed, VEGFR-2 is expressed on LYVE-1 positive lymphatic vessels at P2.5 (Fig

20   S1B) and *Vegf-a* is the most abundantly expressed endothelial growth factor in the post-

21   natal diaphragm at P2.5 (Fig 1F). We therefore treated neonates from P0.5-3.5 with Cmpd

22   31 (20 mg/kg/day i.p.) with or without 3 mg/kg/day of 4G3, a VEGF-A neutralizing antibody

23   (Poor et al., 2014). The analysis of P4.5 LYVE1 immuno-stained diaphragms revealed

10

1   that VEGF-A neutralization alone had no detectable effect on lymphatic vessel parame-

2   ters in the present model, as expected from earlier experiments (Zhang et al., 2018).

3   However, VEGF-A neutralization mildly reduced the Cmpd 31-mediated increase in

4   LYVE1+ lymphatic vessel area and entirely abolished both the Cmpd 31-induced enlarge-

5   ment of lymphatic vessel diameter and LEC proliferation (Fig 1B-E,G,H). None of the

6   tested treatments significantly affected vessel branch formation. Cmpd 31 also increased

7   lymphatic vessel area in the abdominal skin with a trend of reduction by co-treatment with

8   4G3 (Fig S1C). Hence, we report that enhanced S1P signaling enlarges lymphatic vessel

9   diameters and boosts LEC proliferation in a VEGF-A-dependent manner *in vivo*, without

10 affecting vessel branching.

11

12 *Lymphatic endothelial cell S1PR1 signaling reduces lymphatic vessel sprouting inde-*

13 *pendently of VEGF-A*

14 To complement our pharmacological approach of investigating S1P signaling, we used

15 the specific S1PR1 competitive antagonist NIBR0213 (Quancard et al., 2012) during early

16 postnatal lymphangiogenesis. We treated pups from P0.5 to P3.5 i.p. with 10 mg/kg/day

17 of NIBR0213 and sacrificed them at P4.5. At this time point, all NIBR0213 -treated pups

18 had developed chylus ascites, indicative of malfunctioning lymphatic vessels (Fig 2A).

19 Interestingly, analyses of diaphragm whole mounts showed that inhibition of S1PR1 *in*

20 *vivo* only mildly reduced LEC proliferation and had no effect on LYVE1-positive lymphatic

21 vessel area, the total lymphatic vessel network expansion or the calculated lymphatic

22 vessel diameter (Fig 2B, Fig S2A). However, NIBR0213 led to a strong, dose-dependent

1   increase in branch formation (Fig 2B, Fig S2B) and enhanced filopodia formation (Fig 2B,

2   Fig S2C), suggesting that S1PR1 activity inhibits LEC migratory, filopodia-forming re-

3   sponses *in vivo*. Neutralization of VEGF-A did not alter NIBR0213-mediated enhanced

4   branch formation (Fig S2D, E).

5   To demonstrate that the effects of S1PR1 antagonism are indeed intrinsic to LECs we

6   used an inducible genetic loss-of-function approach to delete *S1pr1* specifically in this

7   cell type. Homozygous *S1pr1* flx and *Prox-1-CreERT2+* or *Prox-1-CreERT2-* littermates

8   were treated intragastrically from P1-4 with 50 μg/day tamoxifen and diaphragms were

9   harvested at P7. Analyses of diaphragm whole mounts revealed that, compared to ho-

10 mozygous *S1pr1* flx and *Prox-1-CreERT2-* control pups, S1PR1 was strongly decreased

11 on LYVE1+ lymphatic vessels in homozygous *S1pr1* flx and *Prox-1-CreERT2+* (S1PR1-

12 iΔLEC) littermates, while the S1PR1 expression on blood vessels remained intact (Fig

13 S2F). Importantly, the lymphatic endothelial cell-specific S1PR1 loss-of-function recapit-

14 ulated the phenotypes caused by NIBR0213 treatment. Lymphatic vessel branching and

15 filopodia formation were strongly increased whereas no changes in lymphatic vessel di-

16 ameter and LEC proliferation were found (Fig 2C, D, Fig S2G). Deficiency of LEC S1PR1

17 led to a decreased lymphatic network expansion, suggesting that lymphatic vessel growth

18 was inefficient (Fig 2C). Superficial lymphatic vasculature in the dermis likewise showed

19 increased branch formation, implying a systemic and not an organ-specific effect (Fig 2E).

20 Thus, LEC-specific S1PR1 signaling strongly inhibits lymphatic endothelial cell filopodia

21 formation and vessel branching and is required for a balanced expansion and proper

22 function of the lymphatic vasculature during postnatal development.

23

1 *Lymphatic endothelial cells in vitro exhibit autocrine and constitutive S1P-S1PR1 signal-*

2 *ing.*

3 To study the molecular mechanism by which S1P regulates lymphatic vessel develop-

4 ment, we characterized S1P production and signaling in primary human dermal lymphatic

5 endothelial cells *in vitro*. Liquid chromatography–mass spectrometry analyses of LEC-

6 conditioned medium showed that LECs secrete high amounts of S1P (Fig 3A). Treatment

7 with SKI-II, an inhibitor of sphingosine kinases 1+2 that phosphorylate sphingosine to

8 S1P, completely abolished S1P production. Of note, we showed that already plain, un-

9 conditioned commercial endothelial growth medium (PromoCell EGM-MV) contains ca. 6

10 nM of S1P (Fig 3A) and conclude that active concentration of S1P is constantly present

11 in regular LEC *in vitro* culture.

12 Next, we assessed whether S1P can act on LECs directly in an autocrine manner by

13 measuring endothelial barrier function, a process known to be modulated by S1P (Xiong

14 and Hla, 2014), using electric cell-substrate impedance sensing (ECIS) with high temporal

15 resolution. Inhibition of autocrine S1P production by SKI-II treatment led to the destabili-

16 zation of the LEC barrier and this effect could be overcome by the addition of exogenous

17 S1P (Fig 3B). We then used the competitive and selective antagonist NIBR0213 and

18 showed that S1P-induced barrier stabilization was fully reversed, demonstrating the in-

19 volvement of S1PR1. NIBR0213 is not toxic for LECs as excess S1P could compete for

20 S1PR1 binding and overcome NIBR0213-induced barrier opening (Fig S3). Thus, LECs

21 produce S1P that acts via S1PR1 in an autocrine and constitutive signaling loop that

13

1   manifests in LEC barrier function regulation. Furthermore, LECs expressed S1PR1 pro-

2   tein that was internalized upon stimulation with a saturating concentration of 1 μM exog-

3   enous S1P (Fig 3C).

4

5   *The mitogenic effect of VEGF-A on lymphatic endothelial cells in vitro depends on S1P-*

6   *S1PR1 signaling*

7   In order to gain a better mechanistic understanding of the interaction between VEGF-A

8   and S1P signaling resulting in the enlarged lymphatic vessel diameters and LEC prolifer-

9   ation *in vivo*, we studied VEGF-A-mediated proliferation of human dermal LECs *in* vitro in

10   the presence or absence of S1PR1 signaling. VEGF-A at 100 ng/ml significantly in-

11   creased cell proliferation as determined by EdU incorporation, and strikingly, this effect

12   was completely inhibited by NIBR0213 (Fig 4A). Thus, S1PR1 signaling is required for

13   VEGF-A-mediated LEC proliferation *in vitro*.

14

15   *Autocrine S1P-S1PR1 signaling controls VEGF-A-induced ERK1/2 activation.*

16   We went on to study growth factor-induced ERK1/2 activation *in vitro*, a highly relevant

17   signaling node for mitogenesis in general (Simons et al., 2016) and for VEGF-A down-

18   stream activity in particular (Wang et al., 2010). Using a high throughput homogeneous

19   time resolved fluorescence (HTRF) approach, we determined the phospho-ERK1/2

20   (pERK1/2) response after 10 minutes of titrated VEGF-A with and without NIBR0213 (Fig

21   4B). Indeed, NIBR0213 inhibited pERK1/2 activation mediated by VEGF-A and caused a

14

1   significant increase in EC_{50} of VEGF-A and strongly decreased the Emax of VEGF-A

2   down to 50% (Table 1). Thus, we conclude that VEGF-A-induced ERK1/2 activation is

3   strongly dependent on S1PR1 signaling. Furthermore, at 10ng/ml VEGF-A, a sub-satu-

4   rating concentration, the addition of exogenous S1P significantly increased growth factor-

5   induced ERK1/2 activation (Fig S4A). Hence, S1P-S1PR1 signaling enhances and

6   S1PR1 antagonism limits VEGF-A-mediated ERK1/2 activation in LECs *in vitro.*

7   A positive signaling cross-talk between S1PR1 and VEGFR-2 in LECs was unexpected

8   as earlier work in HUVECs suggested a decrease of VEGF-A-induced pERK1/2 levels

9   (Gaengel et al., 2012). We therefore carried out experiments with human umbilical vein

10   endothelial cells (HUVECs) and obtained results similar to the ones reported here for

11   LECs. Addition of exogenous S1P 1 h prior to or simultaneously with VEGF-A increased

12   pERK1/2 levels and NIBR0213 significantly reduced the signal (Fig S4B).

13   To further confirm that growth factor-induced ERK1/2 activation depends on autocrine

14   production of S1P we assessed the pERK1/2 response after VEGF-A treatments in the

15   presence of the sphingosine kinase inhibitor SKI-II (Fig 4C). With SKI-II, VEGF-A was not

16   able to induce ERK1/2 activation significantly compared to control. Co-stimulation with

17   exogenous S1P overcame the SKI-II block for VEGF-A and significantly increased

18   pERK1/2 levels compared to VEGF-A alone (Fig 4C). This increase was inhibited by

19   S1PR1 antagonism.

20   Taken together, these results show that VEGF-A-induced ERK1/2 activation strongly de-

21   pends on autocrine S1P-S1PR1 signaling.

22

1   *VEGF-A-induced VEGFR-2 trafficking to the perinuclear area depends on S1P-S1PR1*

2   *activity*

3   To investigate how S1P-S1PR1 affects VEGF-A-mediated signaling events, we studied

4   VEGFR-2 phosphorylation and intracellular trafficking following VEGF-A treatment with

5   or without pharmacological S1P pathway modulation. These events, together with recep-

6   tor internalization, were described to be critical for growth factor action (Simons et al.,

7   2016; Wang et al., 2010). Similarly, S1PR1 receptor internalization, trafficking to peri-

8   nuclear area and persistent signaling from intracellular compartments, were demon-

9   strated to be relevant for endothelial barrier regulation (Mullershausen et al., 2009). As

10   shown in Fig. 5A, VEGF-A significantly increased VEGFR-2 Tyr1175 phosphorylation that

11   was unaffected by the S1PR1 antagonist NIBR0213 at all tested time points and VEGF-

12   A concentrations. This indicates that S1P-S1PR1 is not involved in the initial steps of

13   VEGFR-2 signaling, i.e. receptor dimer formation and autophosphorylation. We next as-

14   sessed whether NIBR0213 co-treatment affected VEGFR-2 co-localization with Rab5, an

15   early endosome marker. The co-localization was similar with NIBR0213 co-treatment

16   compared to VEGF-A alone at all tested time points (Fig S5). However, further onward

17   VEGFR-2 trafficking to the perinuclear region was significantly reduced by NIBR0213 co-

18   treatment compared to VEGF-A alone after 10, 20 and 30 min of treatment (Fig 5B, C).

19   These data show that S1P-S1PR1 signaling is not required for VEGFR-2 trafficking to the

20   early endosome but for VEGF-A-mediated VEGFR-2 trafficking to the perinuclear region.

1 **Discussion**

2 Studies have demonstrated that S1P-S1PR1 signaling is required for development and

3 homeostasis of blood vessels (Ben Shoham et al., 2012; Gaengel et al., 2012; Jung et

4 al., 2012). In addition, a signaling cross talk between VEGFR-2 and S1PR1 was reported

5 in blood endothelial cells (Gaengel et al., 2012). However, in the past different groups

6 have drawn differing conclusions on whether S1P has a pro- or anti-angiogenic role (Ben

7 Shoham et al., 2012; Caballero et al., 2009; English et al., 2001; English et al., 2000;

8 Gaengel et al., 2012; Licht et al., 2003). For lymphatic vessels, effect of S1P on patterning

9 was described (Pham et al., 2010), and a matrigel implant *in vivo* model suggested an

10 overall pro-lymphangiogenic effect (Yoon et al., 2008). While it appeared likely that

11 S1PR1 represents the receptor transducing S1P effects in LECs similar to BECs, there

12 was no clear demonstration of this from earlier studies.

13 This study shows, for the first time, that S1P-S1PR1 activity affects lymphangiogenesis

14 by promoting VEGF-A–dependent LEC proliferation and by limiting LEC migratory and

15 filopodia-forming responses *in vivo*. Filopodia formation and proliferation are hallmarks of

16 endothelial tip and stalk cells, respectively. These cell phenotypes are key players in vas-

17 cular patterning, and thus we suggest that the vascular network morphology is critically

18 dependent on tightly controlled S1P-S1PR1 signaling.

19 While it was previously shown that S1PR1 signaling limits migratory, filopodia-forming

20 responses during blood vessel development (Ben Shoham et al., 2012; Gaengel et al.,

21 2012; Jung et al., 2012), a striking synergistic action of S1P with VEGF-A in stimulating

22 cell proliferation, resulting in lymphatic vessel enlargement *in vivo,* was not yet shown

17

1 and is surprising. As earlier studies demonstrated that VEGF-C/VEGFR-3 signaling is

2 required for lymphangiogenesis during the first days after birth (Karpanen et al., 2006;

3 Ochsenbein et al., 2016), we conclude that elevated S1P amplifies VEGF-A signaling in

4 addition to ongoing VEGF-C growth factor signals. Therefore, under physiological condi-

5 tions, VEGF-C signaling does not saturate LEC proliferation, which can be further en-

6 hanced by combined action of VEGF-A and S1P. In support of this, ectopic expression of

7 VEGF-A was shown to increase proliferation rather than migration and filopodia-formation

8 of LECs (Nagy et al., 2002; Wirzenius et al., 2007). Likewise, neutralization of VEGF-A

9 alone in our developing diaphragm model, in the absence of enhanced S1P signaling,

10 had no effect on assessed morphological parameters. This finding is in line with previ-

11 ously published results (Ochsenbein et al., 2016; Zhang et al., 2018), where genetic or

12 antibody-mediated loss of VEGFR-2 signaling had no impact on postnatal lymphangio-

13 genesis.

14 Inhibition of S1PR1 signaling with the specific antagonist NIBR0213 led to chylus ascites

15 formation and increased filopodia formation as well as branch formation *in vivo*, demon-

16 strating dysfunctional and malformed lymphatic vessels. A similar phenotype was ob-

17 tained in animals where S1PR1 was specifically deleted in LECs, emphasizing the im-

18 portant LEC-intrinsic signaling role of S1P/S1PR1. Of note, our data are well in line with

19 a previous report showing increased filopodia formation in mice with lymphatic endothelial

20 cell-specific depletion of sphingosine kinase, which is needed for the generation of S1P

21 (Pham et al., 2010). Furthermore, as increased filopodia-formation is also seen in

22 S1PR1-deficient blood vessels, our data establish a pan-endothelial mechanism.

1   For lymphatics we postulate that S1PR1-mediated inhibition of sprouting acts on alter-

2   native growth factor-driven lymphangiogenic processes, independent of VEGF-A. Earlier

3   work showed that VEGF-C is a crucial driver of postnatal lymphangiogenesis (Zarkada et

4   al., 2015; Zhang et al., 2018) and it will be interesting to investigate how S1P and VEGF-

5   C signaling converge *in vivo* in the future.

6   In order to gain better mechanistic insight into how S1P-S1PR1 affects VEGF-A-mediated

7   lymphangiogenic processes we observed *in vivo*, we characterized S1P-S1PR1 signaling

8   in LECs *in vitro*. We confirmed that S1P-S1PR1 signals in a constitutive and autocrine

9   fashion, as expected from earlier genetic studies showing that LECs generate S1P in a

10   sphingosine kinase 1/2 -dependent manner in mice (Pham et al., 2010). Surprisingly, our

11   *in vitro* data clearly showed that VEGF-A can only signal and exert its mitogenic function

12   when autocrine, constitutive S1P-S1PR1 signaling is active in LECs. The VEGF-A-medi-

13   ated proliferative response of LECs was completely inhibited following blockade of

14   S1PR1. In line with this finding, antagonizing S1PR1 also strongly inhibited VEGF-A –

15   stimulated ERK1/2 activity. Interestingly, 50% of VEGF-A-induced ERK1/2 activity seems

16   to be S1PR1-independent. However, the proliferation data demonstrate that S1PR1-in-

17   dependent ERK1/2 activation is not sufficient to translate into a functional output.

18   A previous report in HUVECs suggested a decrease of VEGF-A-induced pERK1/2 levels

19   with S1P co-treatment (Gaengel et al., 2012). In our experience, HUVECs responded in

20   a similar way to LECs by increasing the pERK1/2 levels. Taken together, we propose that

21   S1P-S1PR1 signaling is a constitutive, LEC-intrinsic mechanism enhancing VEGF-A sig-

22   naling and proliferative function. In line with this conclusion, sphingosine kinases were

19

1 shown to be important for VEGF-A-mediated ERK1/2 activation in retinal blood endothe-

2 lial cells (Maines et al., 2006) and in a bladder tumor cell line (Shu et al., 2002).

3 Upon VEGF-A stimulation, VEGFR-2 is internalized and traffics through different intracel-

4 lular compartments, such as Rab5+ endosomes (Simons et al., 2016). These steps are

5 important for VEGF-A-mediated downstream signaling and aberrant trafficking of

6 VEGFR-2 was shown to decrease ERK1/2 activation (Lanahan et al., 2010). As deficient

7 S1PR1 signaling decreased VEGFR-2 trafficking to the perinuclear region, we speculate

8 that S1PR1–mediated VEGFR-2 trafficking is needed for efficient ERK1/2 activation. Fur-

9 thermore, as S1PR1 antagonism does not impact VEGFR-2 trafficking to Rab5+ early

10 endosomal compartments, we conclude that the crosstalk between VEGFR-2 and S1PR1

11 signaling happens between early endosomes and compartments in the perinuclear re-

12 gion. Interestingly, others have shown that S1PR1 and VEGFR-2 can form signaling com-

13 plexes (Bergelin et al., 2010), and both VEGFR-2 and S1PR1 have been shown to traffic

14 through the same (Rab5+) endosomal compartments (Kofler et al., 2018; Martinez-

15 Morales et al., 2018) relevant for ERK1/2 signaling (Kofler et al., 2018). Furthermore,

16 sphingosine kinases play an important role in endocytotic membrane trafficking in general

17 (Lima et al., 2017; Shen et al., 2014).

18 Interestingly, similar hyperproliferative lymphatic vessel phenotypes as the ones induced

19 by enhanced S1P signaling in our study were described in mice with deficient negative

20 regulators of ERK1/2 signaling, namely SPRED1 and RASA1, as well as for gain-of-func-

21 tion of RAF1, a positive regulator of ERK1/2 (Deng et al., 2013; Lapinski et al., 2012;

22 Taniguchi et al., 2007). Further, lymphatic-specific deletion of the transcription factors

23 FOXC1 and FOXC2 decreased *Rasa3* in embryonic LECs, increased *S1pr1* levels and

1   activated ERK1/2 that resulted in lymphatic vessel enlargement without changes in

2   branching (Fatima et al., 2016). Considering these findings together with our finding that

3   S1P-S1PR1 controls VEGF-A-induced ERK1/2 activation, we suggest that S1P acts as

4   an enhancer of the Ras-Raf-MEK-ERK1/2 signaling cascade upon VEGF-A stimulation

5   *in viv*o, and that negative modulation of S1P-S1PR1 signaling may be beneficial in treat-

6   ing certain genetic diseases linked to lymphatic hyperproliferation.

7   In summary, we show for the first time that autocrine S1P-S1PR1 influences lymphangi-

8   ogenesis by promoting VEGF-A-dependent LEC proliferation and by limiting migratory

9   and filopodia-forming responses. By doing so, S1P-S1PR1 signaling may favor genera-

10   tion of proliferative stalk cells over filopodia-forming tip cells. In line with this notion,

11   S1PR1 negative blood endothelial cells preferably acquire a tip cell position in the growing

12   retinal vasculature (Gaengel et al., 2012). The novel mechanistic insight into the modula-

13   tion of VEGF-A-mediated lymphangiogenesis provided here could be relevant for the un-

14   derstanding of diseases characterized by prominent hyperplastic lymphatic vessels and

15   loss of lymphatic function such as RASopathies.

16

1 **Author contributions**

2 A.M.G.O., G.J. and K.S. designed experiments and A.M.G.O. wrote the paper with sup-

3 port of G.J. and K.S.; G.J. and K.S. supervised the study; A.M.G.O., B.W., S.V. and C.B.

4 performed experiments and A.M.G.O. analyzed data; C.G., L.C., S.L. supported perfor-

5 mance of experiments and experimental design; N.H. wrote the personalized Fiji macro

6 and helped with picture processing.

7

8

1 **Acknowledgements**

7

23

1 **Funding**

24

References

Allende, M. L., Yamashita, T. and Proia, R. L. (2003). G-protein-coupled receptor S1P1 acts within endothelial cells to regulate vascular maturation. *Blood* **102**, 3665-3667.

Bazigou, E., Lyons, O. T., Smith, A., Venn, G. E., Cope, C., Brown, N. A. and Makinen, T. (2011). Genes regulating lymphangiogenesis control venous valve formation and maintenance in mice. *J Clin Invest* **121**, 2984-2992.

Ben Shoham, A., Malkinson, G., Krief, S., Shwartz, Y., Ely, Y., Ferrara, N., Yaniv, K. and Zelzer, E. (2012). S1P1 inhibits sprouting angiogenesis during vascular development. *Development* **139**, 3859-3869.

Berdyshev, E. V., Gorshkova, I. A., Garcia, J. G., Natarajan, V. and Hubbard, W. C. (2005). Quantitative analysis of sphingoid base-1-phosphates as bisacetylated derivatives by liquid chromatography-tandem mass spectrometry. *Anal Biochem* **339**, 129-136.

Bergelin, N., Lof, C., Balthasar, S., Kalhori, V. and Tornquist, K. (2010). S1P1 and VEGFR-2 form a signaling complex with extracellularly regulated kinase 1/2 and protein kinase C-alpha regulating ML-1 thyroid carcinoma cell migration. *Endocrinology* **151**, 2994-3005.

Bigaud, M., Dincer, Z., Bollbuck, B., Dawson, J., Beckmann, N., Beerli, C., Fishli-Cavelti, G., Nahler, M., Angst, D., Janser, P., et al. (2016). Pathophysiological Consequences of a Break in S1P1-Dependent Homeostasis of Vascular Permeability Revealed by S1P1 Competitive Antagonism. *PLoS One* **11**, e0168252.

Billich, A., Baumruker, T., Beerli, C., Bigaud, M., Bruns, C., Calzascia, T., Isken, A., Kinzel, B., Loetscher, E., Metzler, B., et al. (2013). Partial deficiency of sphingosine-1-phosphate lyase confers protection in experimental autoimmune encephalomyelitis. *PLoS One* **8**, e59630.

Caballero, S., Swaney, J., Moreno, K., Afzal, A., Kielczewski, J., Stoller, G., Cavalli, A., Garland, W., Hansen, G., Sabbadini, R., et al. (2009). Anti-sphingosine-1-phosphate monoclonal antibodies inhibit angiogenesis and sub-retinal fibrosis in a murine model of laser-induced choroidal neovascularization. *Exp Eye Res* **88**, 367-377.

Deng, Y., Atri, D., Eichmann, A. and Simons, M. (2013). Endothelial ERK signaling controls lymphatic fate specification. *J Clin Invest* **123**, 1202-1215.

English, D., Garcia, J. G. and Brindley, D. N. (2001). Platelet-released phospholipids link haemostasis and angiogenesis. *Cardiovasc Res* **49**, 588-599.

English, D., Welch, Z., Kovala, A. T., Harvey, K., Volpert, O. V., Brindley, D. N. and Garcia, J. G. (2000). Sphingosine 1-phosphate released from platelets during clotting accounts for the potent endothelial cell chemotactic activity of blood serum and provides a novel link between hemostasis and angiogenesis. *FASEB J* **14**, 2255-2265.

Fatima, A., Wang, Y., Uchida, Y., Norden, P., Liu, T., Culver, A., Dietz, W. H., Culver, F., Millay, M., Mukouyama, Y. S., et al. (2016). Foxc1 and Foxc2 deletion causes abnormal lymphangiogenesis and correlates with ERK hyperactivation. *J Clin Invest* **126**, 2437-2451.

Gaengel, K., Niaudet, C., Hagikura, K., Lavina, B., Muhl, L., Hofmann, J. J., Ebarasi, L., Nystrom, S., Rymo, S., Chen, L. L., et al. (2012). The sphingosine-1-phosphate receptor S1PR1 restricts sprouting angiogenesis by regulating the interplay between VE-cadherin and VEGFR2. *Dev Cell* **23**, 587-599.

Gerhardt, H., Golding, M., Fruttiger, M., Ruhrberg, C., Lundkvist, A., Abramsson, A., Jeltsch, M., Mitchell, C., Alitalo, K., Shima, D., et al. (2003). VEGF guides angiogenic sprouting utilizing endothelial tip cell filopodia. *J Cell Biol* **161**, 1163-1177.

James, J. M., Nalbandian, A. and Mukouyama, Y. S. (2013). TGFbeta signaling is required for sprouting lymphangiogenesis during lymphatic network development in the skin. *Development* **140**, 3903-3914.

Jung, B., Obinata, H., Galvani, S., Mendelson, K., Ding, B. S., Skoura, A., Kinzel, B., Brinkmann, V., Rafii, S., Evans, T., et al. (2012). Flow-regulated endothelial S1P receptor-1 signaling sustains vascular development. *Dev Cell* **23**, 600-610.

Karpanen, T., Wirzenius, M., Makinen, T., Veikkola, T., Haisma, H. J., Achen, M. G., Stacker, S. A., Pytowski, B., Yla-Herttuala, S. and Alitalo, K. (2006). Lymphangiogenic growth factor responsiveness is modulated by postnatal lymphatic vessel maturation. *Am J Pathol* **169**, 708-718.

Kofler, N., Corti, F., Rivera-Molina, F., Deng, Y., Toomre, D. and Simons, M. (2018). The Rab-effector protein RABEP2 regulates endosomal trafficking to mediate vascular endothelial growth factor receptor-2 (VEGFR2)-dependent signaling. *Journal of Biological Chemistry* **293**, 4805-4817.

Lanahan, A. A., Hermans, K., Claes, F., Kerley-Hamilton, J. S., Zhuang, Z. W., Giordano, F. J., Carmeliet, P. and Simons, M. (2010). VEGF receptor 2 endocytic trafficking regulates arterial morphogenesis. *Dev Cell* **18**, 713-724.

Lapinski, P. E., Kwon, S., Lubeck, B. A., Wilkinson, J. E., Srinivasan, R. S., Sevick-Muraca, E. and King, P. D. (2012). RASA1 maintains the lymphatic vasculature in a quiescent functional state in mice. *J Clin Invest* **122**, 733-747.

Licht, T., Tsirulnikov, L., Reuveni, H., Yarnitzky, T. and Ben-Sasson, S. A. (2003). Induction of pro-angiogenic signaling by a synthetic peptide derived from the second intracellular loop of S1P3 (EDG3). *Blood* **102**, 2099-2107.

Lima, S., Milstien, S. and Spiegel, S. (2017). Sphingosine and Sphingosine Kinase 1 Involvement in Endocytic Membrane Trafficking. *J Biol Chem* **292**, 3074-3088.

Maines, L. W., French, K. J., Wolpert, E. B., Antonetti, D. A. and Smith, C. D. (2006). Pharmacologic manipulation of sphingosine kinase in retinal endothelial cells: implications for angiogenic ocular diseases. *Invest Ophthalmol Vis Sci* **47**, 5022-5031.

Martinez-Morales, J. C., Romero-Avila, M. T., Reyes-Cruz, G. and Garcia-Sainz, J. A. (2018). S1P1 receptor phosphorylation, internalization, and interaction with Rab proteins: effects of sphingosine 1-phosphate, FTY720-P, phorbol esters, and paroxetine. *Biosci Rep* **38**.

Mullershausen, F., Zecri, F., Cetin, C., Billich, A., Guerini, D. and Seuwen, K. (2009). Persistent signaling induced by FTY720-phosphate is mediated by internalized S1P1 receptors. *Nat Chem Biol* **5**, 428-434.

Nagy, J. A., Vasile, E., Feng, D., Sundberg, C., Brown, L. F., Detmar, M. J., Lawitts, J. A., Benjamin, L., Tan, X., Manseau, E. J., et al. (2002). Vascular permeability factor/vascular endothelial growth factor induces lymphangiogenesis as well as angiogenesis. *J Exp Med* **196**, 1497-1506.

Ochsenbein, A. M., Karaman, S., Proulx, S. T., Goldmann, R., Chittazhathu, J., Dasargyri, A., Chong, C., Leroux, J. C., Stanley, E. R. and Detmar, M. (2016). Regulation of lymphangiogenesis in the diaphragm by macrophages and VEGFR-3 signaling. *Angiogenesis* **19**, 513-524.

Pham, T. H., Baluk, P., Xu, Y., Grigorova, I., Bankovich, A. J., Pappu, R., Coughlin, S. R., McDonald, D. M., Schwab, S. R. and Cyster, J. G. (2010). Lymphatic endothelial cell sphingosine kinase activity is required for lymphocyte egress and lymphatic patterning. *J Exp Med* **207**, 17-27.

Poor, S. H., Qiu, Y., Fassbender, E. S., Shen, S., Woolfenden, A., Delpero, A., Kim, Y., Buchanan, N., Gebuhr, T. C., Hanks, S. M., et al. (2014). Reliability of the mouse model of choroidal neovascularization induced by laser photocoagulation. *Invest Ophthalmol Vis Sci* **55**, 6525-6534.

1 **Preibisch, S., Saalfeld, S. and Tomancak, P.** (2009). Globally optimal stitching of tiled 3D
2   microscopic image acquisitions. *Bioinformatics* **25**, 1463-1465.
3 **Quancard, J., Bollbuck, B., Janser, P., Angst, D., Berst, F., Buehlmayer, P., Streiff, M.,**
4   **Beerli, C., Brinkmann, V., Guerini, D., et al.** (2012). A potent and selective S1P(1)
5   antagonist with efficacy in experimental autoimmune encephalomyelitis. *Chem Biol* **19**,
6   1142-1151.
7 **Ridler, T. W. and Calvard, S.** (1978). Picture Thresholding Using an Iterative Selection Method.
8   *Ieee T Syst Man Cyb* **8**, 630-632.
9 **Rueden, C. T., Schindelin, J., Hiner, M. C., DeZonia, B. E., Walter, A. E., Arena, E. T. and**
10   **Eliceiri, K. W.** (2017). ImageJ2: ImageJ for the next generation of scientific image data.
11   *BMC Bioinformatics* **18**, 529.
12 **Schindelin, J., Arganda-Carreras, I., Frise, E., Kaynig, V., Longair, M., Pietzsch, T.,**
13   **Preibisch, S., Rueden, C., Saalfeld, S., Schmid, B., et al.** (2012). Fiji: an open-source
14   platform for biological-image analysis. *Nat Methods* **9**, 676-682.
15 **Shen, H. Y., Giordano, F., Wu, Y. M., Chan, J., Zhu, C., Milosevic, I., Wu, X. D., Yao, K.,**
16   **Chen, B., Baumgart, T., et al.** (2014). Coupling between endocytosis and sphingosine
17   kinase 1 recruitment. *Nature Cell Biology* **16**, 652-+.
18 **Shu, X., Wu, W., Mosteller, R. D. and Broek, D.** (2002). Sphingosine kinase mediates vascular
19   endothelial growth factor-induced activation of ras and mitogen-activated protein
20   kinases. *Mol Cell Biol* **22**, 7758-7768.
21 **Simons, M., Gordon, E. and Claesson-Welsh, L.** (2016). Mechanisms and regulation of
22   endothelial VEGF receptor signalling. *Nat Rev Mol Cell Biol* **17**, 611-625.
23 **Taniguchi, K., Kohno, R., Ayada, T., Kato, R., Ichiyama, K., Morisada, T., Oike, Y.,**
24   **Yonemitsu, Y., Maehara, Y. and Yoshimura, A.** (2007). Spreds are essential for
25   embryonic lymphangiogenesis by regulating vascular endothelial growth factor receptor
26   3 signaling. *Mol Cell Biol* **27**, 4541-4550.
27 **Vaahtomeri, K., Karaman, S., Makinen, T. and Alitalo, K.** (2017). Lymphangiogenesis
28   guidance by paracrine and pericellular factors. *Genes Dev* **31**, 1615-1634.
29 **Wang, Y., Nakayama, M., Pitulescu, M. E., Schmidt, T. S., Bochenek, M. L., Sakakibara, A.,**
30   **Adams, S., Davy, A., Deutsch, U., Luthi, U., et al.** (2010). Ephrin-B2 controls VEGF-
31   induced angiogenesis and lymphangiogenesis. *Nature* **465**, 483-486.
32 **Weiler, S., Braendlin, N., Beerli, C., Bergsdorf, C., Schubart, A., Srinivas, H., Oberhauser,**
33   **B. and Billich, A.** (2014). Orally active 7-substituted (4-benzylphthalazin-1-yl)-2-
34   methylpiperazin-1-yl]nicotinonitriles as active-site inhibitors of sphingosine 1-phosphate
35   lyase for the treatment of multiple sclerosis. *J Med Chem* **57**, 5074-5084.
36 **Wirzenius, M., Tammela, T., Uutela, M., He, Y., Odorisio, T., Zambruno, G., Nagy, J. A.,**
37   **Dvorak, H. F., Yla-Herttuala, S., Shibuya, M., et al.** (2007). Distinct vascular
38   endothelial growth factor signals for lymphatic vessel enlargement and sprouting. *J Exp*
39   *Med* **204**, 1431-1440.
40 **Xiong, Y. and Hla, T.** (2014). S1P control of endothelial integrity. *Curr Top Microbiol Immunol*
41   **378**, 85-105.
42 **Yanagida, K. and Hla, T.** (2017). Vascular and Immunobiology of the Circulatory Sphingosine
43   1-Phosphate Gradient. *Annu Rev Physiol* **79**, 67-91.
44 **Yoon, C. M., Hong, B. S., Moon, H. G., Lim, S., Suh, P. G., Kim, Y. K., Chae, C. B. and Gho,**
45   **Y. S.** (2008). Sphingosine-1-phosphate promotes lymphangiogenesis by stimulating
46   S1P1/Gi/PLC/Ca2+ signaling pathways. *Blood* **112**, 1129-1138.
47 **Zarkada, G., Heinolainen, K., Makinen, T., Kubota, Y. and Alitalo, K.** (2015). VEGFR3 does
48   not sustain retinal angiogenesis without VEGFR2. *P Natl Acad Sci USA* **112**, 761-766.
49 **Zhang, X. and Simons, M.** (2014). Receptor Tyrosine Kinases Endocytosis in Endothelium
50   Biology and Signaling. *Arterioscl Throm Vas* **34**, 1831-1837.

1   **Zhang, Y., Ulvmar, M. H., Stanczuk, L., Martinez-Corral, I., Frye, M., Alitalo, K. and**
2   **Makinen, T.** (2018). Heterogeneity in VEGFR3 levels drives lymphatic vessel
3   hyperplasia through cell-autonomous and non-cell-autonomous mechanisms. *Nat*
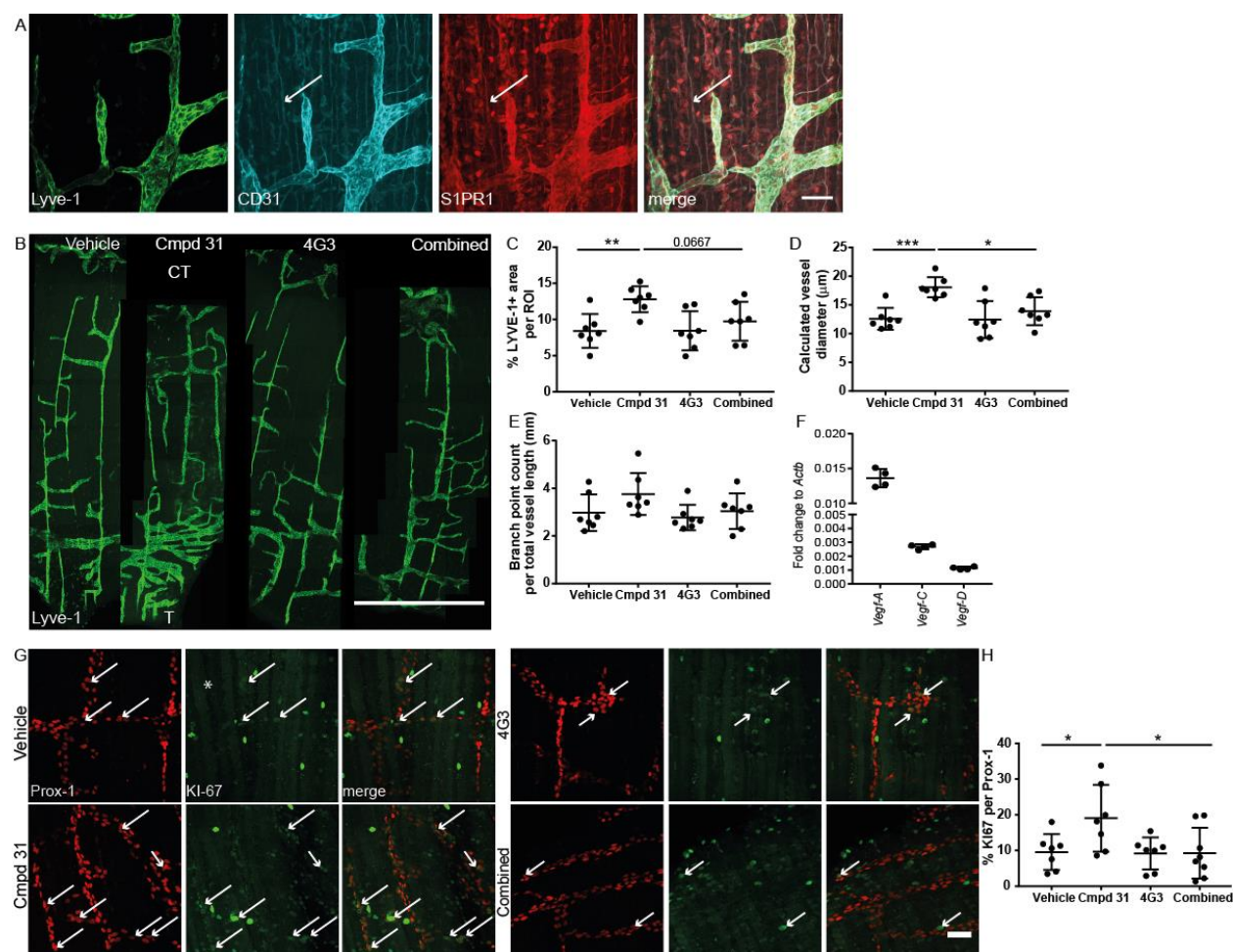4   *Commun* **9**, 1296.

5

6

1   **Figures with Figure legends**

2

3   **Figure 1: S1P enhances LEC proliferation in a VEGF-A-dependent manner *in vivo*.**
4   A) Representative confocal images of P4.5 diaphragm whole mounts (pleural side)
5   stained for LYVE1 (green), CD31 (blue) and S1PR1 (red). Arrow highlights an example
6   of CD31+ and S1PR1+ blood vessel. Scale bar 50 μm. B) Representative stitched confo-
7   cal images of P4.5 LYVE1-immunostained diaphragm whole mounts (pleural side) of
8   pups exposed to indicated treatments. T= Thorax wall, CT = Central tendon, scale bar 1
9   mm. C-E) Quantification of lymphatic vessel parameters of treated pups. F) Real-time
10   qPCR analysis of lymphatic growth factor gene expressions compared to *Actb* in P2.5
11   diaphragms. G-H) Representative confocal images and quantifications of diaphragm
12   whole mounts immunostained for Prox-1 (red) and KI-67 (green) after indicated treat-
13   ments. Arrows: KI-67 + LECs, scale bar 50 μm. Statistical analyses: Dots represent ani-
14   mal mean, lines represent group means, error bars represent ±SD. Statistical significance
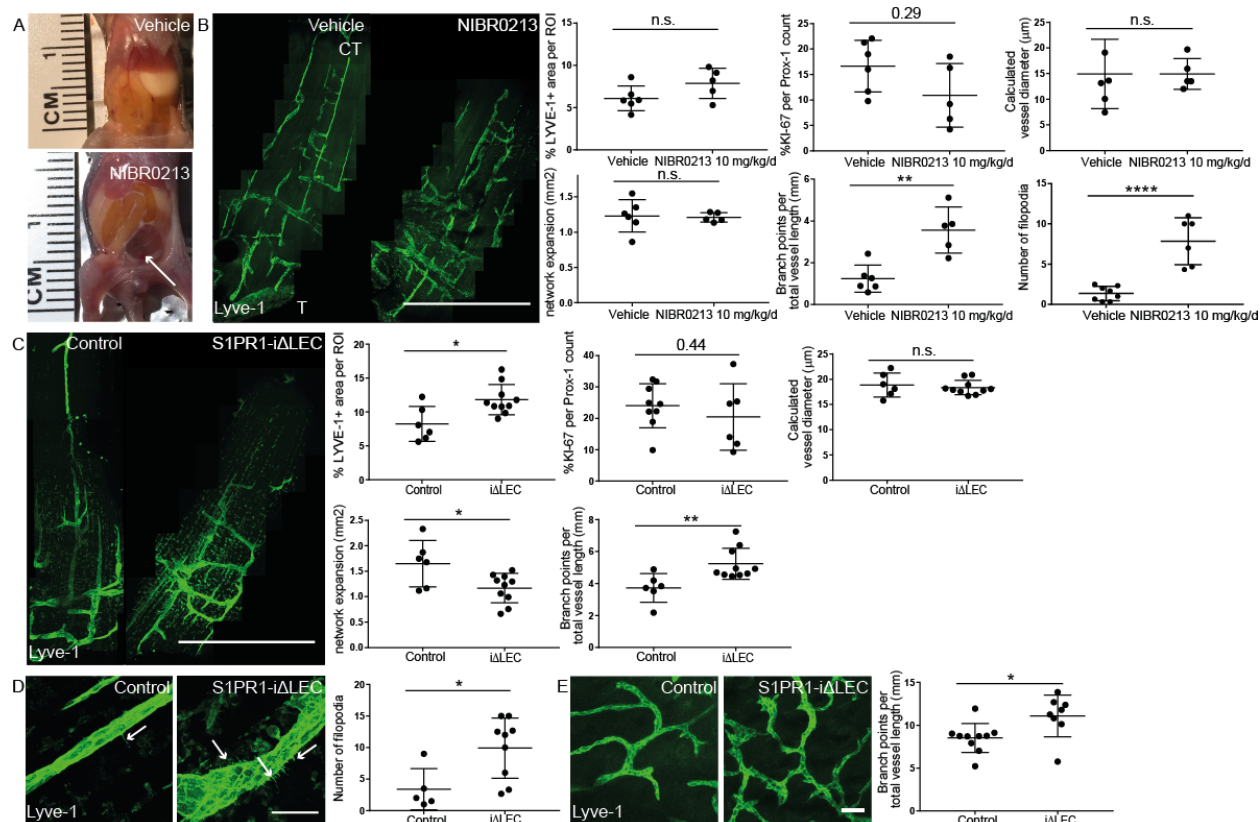15   was calculated with one-way ANOVA and Dunnett's test.

16

Figure 2: S1PR1 in lymphatic endothelial cells reduces filopodia formation and branching. A) Images of P4.5 vehicle and NIBR0213 treated pups with exposed perito-neum. Arrow indicates chylus ascites. B) Stitched confocal images and quantification of lateral segments of LYVE1 immunostained diaphragm whole mounts of vehicle or 10 mg/kg/day NIBR0213 treated pups. CT= Central tendon, T = Thorax wall. Scale bar 1 mm. C) Stitched confocal images and quantification of a lateral segment of LYVE1 im-munostained diaphragm whole mounts of P7 control or S1PR1-iΔLEC pups. Scale bar 1 mm. D) High magnification confocal images and quantification of increased filopodia for-mation of LYVE1 immunostained diaphragmatic lymphatic vessel in control and S1PR1-iΔLEC pups. Arrow indicates filopodia, scale bar 50 μm. E) Confocal images and quanti-fication of LYVE1 immunostained abdominal skin whole mount of P7 control or S1PR1-iΔLEC pups. Scale bar 50 μm. Statistical analysis: Dots represent animal mean, lines represent group means, error bars = ±SD. Statistical significance was calculated using an unpaired Student's t-test, or for C Branch points per vessel length a Mann Whitney test.
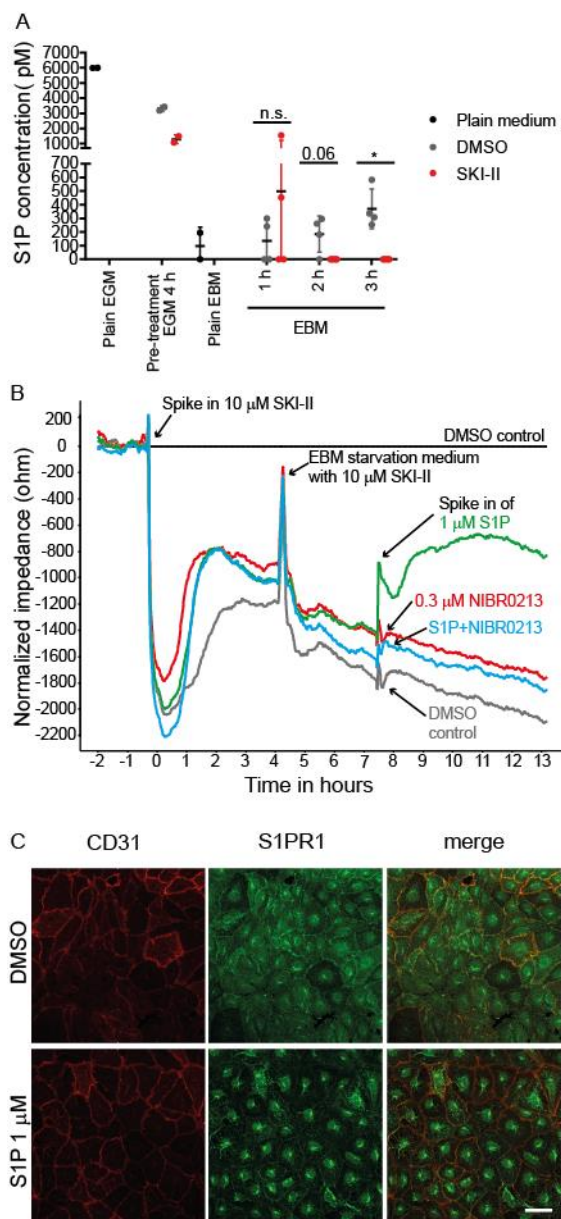
Fig 3: Lymphatic endothelial cells *in vitro* exhibit autocrine and constitutive S1P-S1PR1 signaling. A) S1P concentrations in plain medium (black dots) or in conditioned supernatants of LEC treated ± SKI-II (grey or red dots). B) Normalized (to DMSO control) electrical impedance of LEC monolayers after indicated treatments. C) CD31 (red) and S1PR1 (green) immunofluorescence of LECs monolayer treated with 1 μM S1P for 1 h. Representative confocal images; Scale bar = 50 μm. Statistical analyses: Dots represent individual measurements, lines group means, error bars = ±SD. Statistical significance was calculated using an unpaired Student's t-test and Welch's correction for unequal variances.
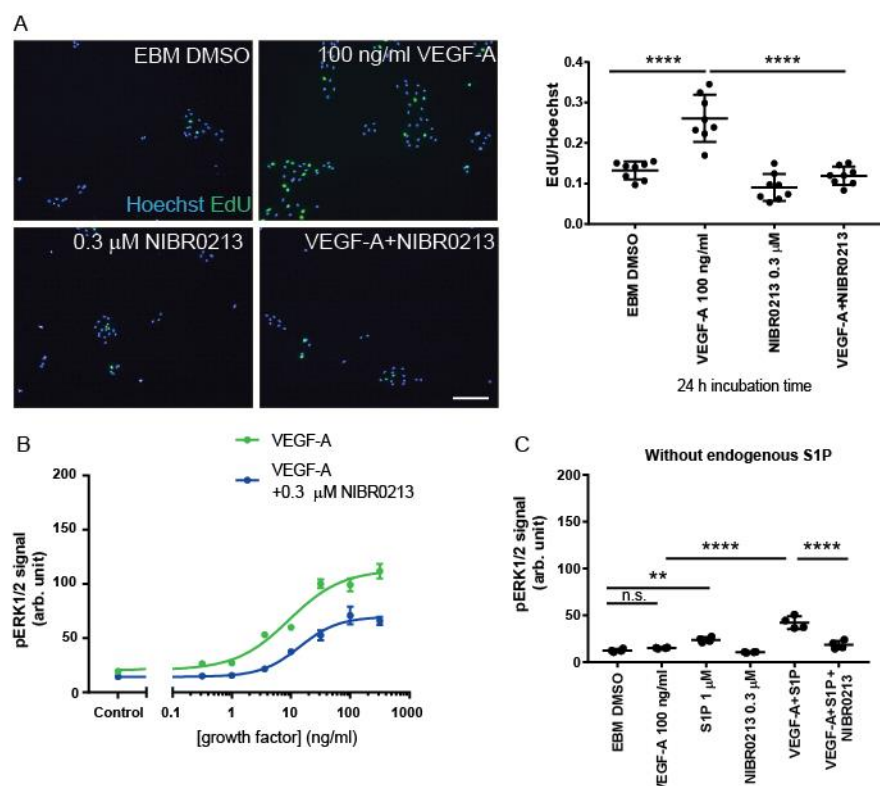
31

1

2

Figure 4: VEGF-A-induced ERK1/2 activation and proliferation depend on autocrine S1P-S1PR1. A) EdU (green) and Hoechst (blue) staining along with quantifications of cultured LEC after 24 h of indicated treatments. Representative images; Scale bar: 200 μm. B,C) Quantification of pERK1/2 levels assessed by HTRF in LEC lysates after 10 min of indicated treatments. Statistical analyses: In A and C, dots represent individual measurements, lines represent group means. In B, dots represent group means, lines represent fitted curves. Error bars = ±SD. Statistical significance was calculated using one-way ANOVA and Dunnett's test.
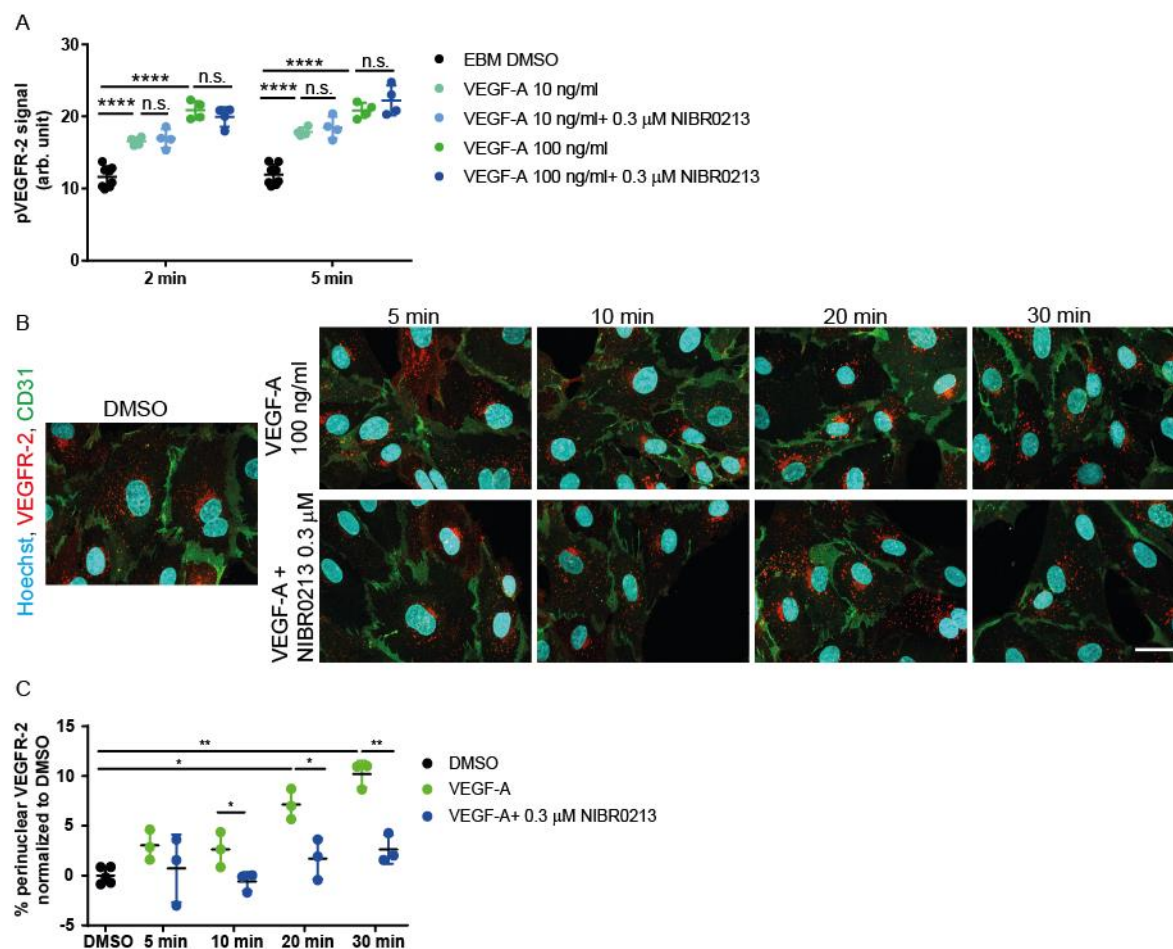
Figure 5: VEGF-A-induced VEGFR-2 translocation to the perinuclear area depends on S1PR1. A) Quantification of pVEGFR-2 levels, assessed by HTRF, in LEC lysates after indicated treatments and incubation times. B,C) Immunofluorescent staining of VEGFR-2 (red), CD31 (green) and Hoechst (blue) and quantification of VEGFR-2 trafficking to the perinuclear area of cultured LEC after indicated treatments and incubation times. Representative confocal images; Scale bars: 50 μm. Statistical analyses: Dots represent individual measurements, lines group means, error bars = ±SD. Statistical significance was calculated using one-way ANOVA and Dunnett's test.

33

1 **Tables**

2 **Table 1: Potency and efficacy parameters for VEGF-A induced ERK1/2 activation.**

Growth factor ± 0.3 μM NIBR0213	EC_{50} (ng/ml) Average±SD, (n)	P value (one –way ANOVA)	EMax (% of VEGF-A) Average±SD, (n)	P value (one –way ANOVA)
VEGF-A	7.56±3.96, (6)		100±20, (7)	
VEGF-A+ NIBR0213	20.29±7.61, (3)	To VEGF-A: 0.0418	55±11, (5)	To VEGF-A: 0.0048

3 Representative fitted curves shown in Fig 4B.

4